Supplementary Information

Nanocluster reaction-driven *in-situ* transformation of colloidal nanoparticles to mesostructures

Paulami Bose,[a†] Pillalamarri Srikrishnarka,[a†] Matias Paatelainen,[b] Nonappa,[b] Amoghavarsha Ramachandra Kini,[a] Anirban Som,[a] and Thalappil Pradeep[a]*

[a]DST Unit of Nanoscience (DST UNS) and Thematic Unit of Excellence (TUE), Department of Chemistry, Indian Institute of Technology Madras, Chennai 600 036, India.

[†b]Faculty of Natural Sciences and Engineering, Tampere University, Korkeakoulunkatu 3, FI-33720, Tampere, Finland

*E-mail: pradeep@iitm.ac.in

[†]Present address

Table of Contents

SI 1. Instrumentation

Instrumentation. *Optical Absorption Spectroscopy:* The optical absorption spectra were recorded using a Perkin Elmer Lambda 25 instrument with a range of 200 – 1100 nm and a bandpass filter of 1 nm.

High-resolution transmission electron microscopy: HRTEM imaging was carried out in JEOL 3010, JEOL JEM F200, and Thermo Scientific Talos 200i instruments. Gatan 794 multiscan CCD, Gatan OneView, and Ceta 16M CMOS cameras were used to capture the images. Samples were prepared by dropcasting the dispersion on carbon-coated copper grids (spi Supplies, 3530C-MB) and dried at ambient conditions.

High-resolution field emission scanning electron microscope: HR FESEM and energy-dispersive X-ray spectroscopy (EDS) imaging were carried out in a Thermo Scientific Verios G4 UC. The instrument is equipped with a Schottky FEG electron gun with an adjustable probe current ranging between 0.8 nA−100 nA. The surface was imaged using backscattered and secondary electrons, with an accelerating voltage of 10 kV and high vacuum conditions.

Optical microscope: Keyence VHX-6000 digital microscope with VH-Z100T field lens (100-1000x) magnification.

Dynamic light scattering: DLS measurements were performed in a glass cuvette (10 mm path length) using a Malvern Zetasizer Nano-ZS instrument.

Atomic Force microscopy: AFM images were collected using a Bruker Dimension Icon instrument. The ScanAsyst mode was utilized for the measurement, using RTESPA-150 and RTESPA-300 probes.

Scanning Transmission Electron Microscopy and EDS mapping: The STEM imaging was performed using a JEOL JEM F200 high throughput electron microscope equipped with a Schottky-type field emission gun operated at 200 kV with simultaneous bright field (BF) and dark field (DF) STEM imaging. Energy-dispersive X-ray mapping and spectra were collected using dual silicon drift detectors.

SI 2. Experimental section

Materials. Silver nitrate ($AgNO_3$, ≥99%), 2-phenylethanethiol (PET, 98%), tetraoctylammonium bromide (TOABr, 98%), 2,4-dimethylbenzenethiol (DMBT, 95%), sodium borohydride ($NaBH_4$, ≥99%), and triphenylphosphine (TPP, 99%) were purchased from Sigma Aldrich. Tetrachloroauric acid ($HAuCl_4.3H_2O$) was prepared from pure gold and aqua regia in the laboratory. All the solvents used were of HPLC grade without further purification. Millipore-produced deionized water (∼18.2 MΩ) was used throughout the experiments.

Synthesis of Ag@PET nanoparticles. 2-PET-capped Ag NPs were synthesized by modifying the traditional preparation method of silver NPs.[1,2] 50 mg of $AgNO_3$ was dissolved in 0.5 mL of water and added to 58 µL of PET in 30 mL of methanol. Next, silver was reduced to the zero-valent state by slowly adding the freshly prepared aqueous $NaBH_4$ solution (75 mg in 8 mL ice-cold water) with vigorous stirring. The reaction mixture was further stirred for an hour, followed by overnight refluxing at 333 K. For purification, the precipitate was collected and repeatedly washed with methanol by centrifugal precipitation. Finally, the purified NPs were extracted in DCM, size-focussed using high-speed centrifugation, dried in a rotary evaporator, and stored in a refrigerator.

The synthesized Au@PET NPs were characterized using optical absorption spectroscopy and HRTEM; the characterization data are presented in Fig. 1B g-I and S2. From the particle size distribution, the NPs were found to have an average size of 4.4 ± 2.3 nm. The most probable diameter of the metallic core of the particle is considered for particle size calculation.

Synthesis of the $[Au_{25}(PET)_{18}]^-$ nanocluster. The NC was synthesized using a slightly modified reported protocol.[3] Initially, a solution of 40 mg of $HAuCl_4 \cdot 3H_2O$ in 7.5 mL of THF was prepared. Next, 65 mg of TOABr was added to the reaction mixture and stirred for 15 min. Then, 68 µL of PET was added, and the mixture was further stirred for an hour, followed by the slow addition of freshly prepared aqueous $NaBH_4$ solution (39 mg in 2.5 mL ice-cold water). The reaction mixture was stirred for another 5 h for a complete reduction and size focussing. For purification, the crude NC solution was centrifuged to remove free thiols and excess thiolates, and the collected supernatant was concentrated by rotary evaporation. The precipitate was washed multiple times with methanol. The NC was extracted in acetone and centrifuged, the supernatant was collected, and the precipitate containing larger NCs was discarded. The supernatant comprising the pure NC was vacuum-dried and finally collected in DCM.

The purified NC was characterized using optical absorption microscopy, HRTEM, and ESI MS (Fig. 1B a-c and S1).

Synthesis of the $[Ag_{25}(DMBT)_{18}]^-$ nanocluster. The NC was synthesized by slightly modifying a previously reported protocol.[4] First, 38.0 mg of $AgNO_3$ was dissolved in 2 mL of methanol. To this mixture, 90 µL of 2,4-DMBT was added, which produced an insoluble yellow Ag-thiolate, followed by 17 mL of DCM, and then it was stirred for 15 mins at 0 °C. Afterwards, 0.5 mL of methanolic solution of 6 mg PPh_4Br was added, followed by a dropwise addition of 15.0 mg of $NaBH_4$ in 0.5 mL of ice-cold water. The reaction mixture was further stirred for 7-8 h, followed by overnight ageing in the refrigerator. For purification, the crude NC solution was centrifuged to remove any insoluble impurities, and the collected supernatant was concentrated by rotary evaporation. The precipitate was washed multiple times with methanol. Then, the NC was extracted in DCM and centrifuged again to remove any remaining insoluble impurities. DCM was removed using rotavapor, and the purified NC was obtained in its powdered form.

Synthesis of Au@DMBT nanoparticles. The synthesis of 2,4-dimethylbenzenethiol-capped Au nanoparticles, referred to as Au@DMBT NPs, was carried out using a modified Brust-Schiffrin synthesis method.[5] Initially, an aqueous $HAuCl_4 \cdot 3H_2O$ (5.0 mg in 0.5 mL H_2O) was mixed with 13.4 mg of TOABr in 30 mL toluene. The aqueous-organic mixture was vigorously stirred for 15 min, and then 7 µL of 2,4-DMBT was added. Next, 2.0 mg of $NaBH_4$ in 10 mL of ice-cold water was added dropwise with vigorous stirring as the color of the reaction mixture turned purple. After stirring the reaction mixture for nearly an hour, the organic layer was separated, and the size focussing was done with overnight heating at 60 °C. After heating, the color of the organic layer changed from purple to wine-red. Further purification was performed by removing the solvent under reduced pressure using a rotary evaporator and washing it with ethanol. Finally, the purified NP was extracted in toluene, dried in a rotary evaporator, and stored in a refrigerator.

The synthesized Au@DMBT NPs were characterized using optical absorption spectroscopy and HRTEM, as presented in Fig. S15. From the particle size distribution, the NPs were found to have an average size of 4.5 ± 0.6 nm. Please note that for particle size calculation, we are referring to the most probable diameter of the metallic core of the particle.

Synthesis of Au@PET nanoparticles. The synthesis of 2-phenylethanethiol-capped Au nanoparticles, referred to as Au@PET NPs, was prepared using a modified Brust-Schiffrin synthesis method.[5] Initially, an aqueous $HAuCl_4 \cdot 3H_2O$ (5.0 mg in 0.5 mL H_2O) was mixed with 13.4 mg of TOABr in 30 mL toluene. The aqueous-organic mixture was vigorously stirred for 15 min, and then 7 µL of 2-PET was added. Next, a freshly prepared aqueous solution of $NaBH_4$ (6.0 mg in 10 mL of ice-cold water) was added dropwise with vigorous stirring as the color of the reaction mixture turned purple. After stirring the reaction mixture for nearly an hour, the organic layer was separated, and the size focussing was done with overnight heating at 60 °C. After heating, the color of the organic layer changed from purple to wine-red. Further purification was performed by removing the solvent under reduced pressure using a rotary evaporator and washing it with ethanol. Finally, the purified NP was extracted in toluene, dried in a rotary evaporator, and stored in a refrigerator.

The synthesized Au@PET NPs were characterized using optical absorption spectroscopy and HRTEM, as presented in Fig. S16.

Nucleation and assembly of mesostructures. For interparticle reaction, 7 mg of Ag@PET NPs were dissolved in 6 mL solvent, and about 0.9 mg of the $Au_{25}(PET)_{18}$ NC was dissolved in 600 µL of solvent, separately. The final reaction mixture was made by combining the NP and NC dispersions at room temperature in a leak-proof reaction bottle and allowing them to react under constant stirring and heating/no heating for an extended period of time (of the order of days); demonstration of the setup in Fig. S5. The reaction was monitored using microscopic (optical, TEM, and FESEM) and spectroscopic (UV-Vis and DLS) techniques.

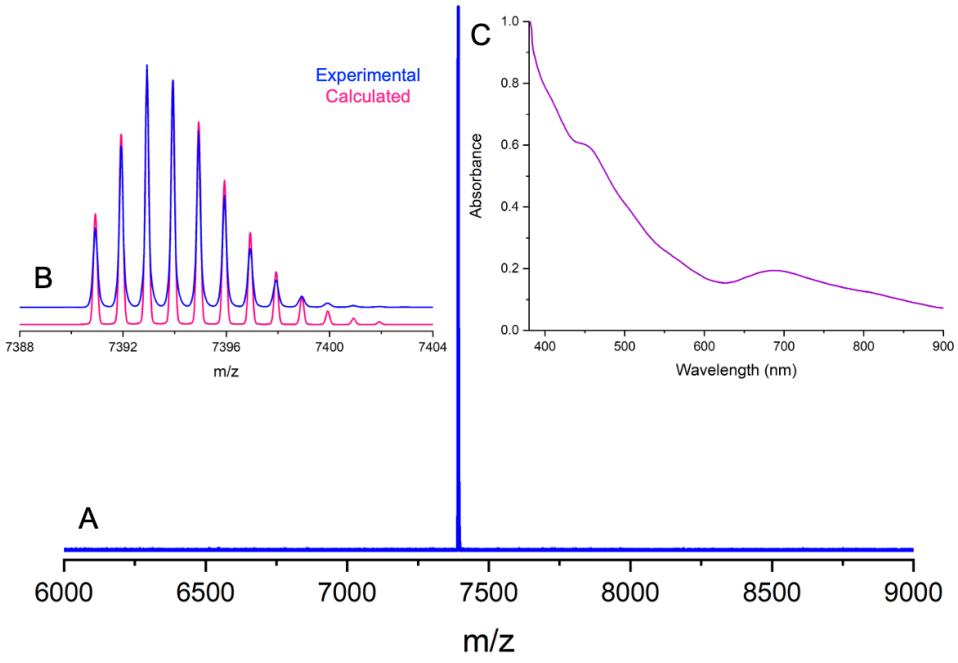

Fig. S1 Characterization of $[Au_{25}(PET)_{18}]^-$ NC. (A) ESI MS of the molecular ion peak, (B) the corresponding experimental and theoretical comparison of the high-resolution isotopic distribution, and (C) optical absorption spectrum.

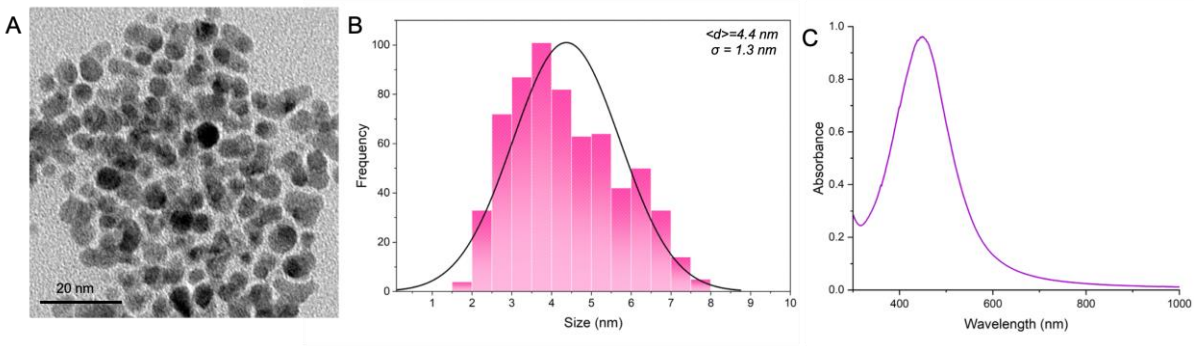

Fig. S2 Characterization of Ag@PET NPs. (A) TEM image, (B) the corresponding particle size distribution, and (C) the optical absorption spectrum of the polydispersed Ag@PET NPs. The terms <d> and σ refer to the mean diameter and standard deviation, respectively. Note that the most probable diameter of the metal core is considered for the estimation of particle size.

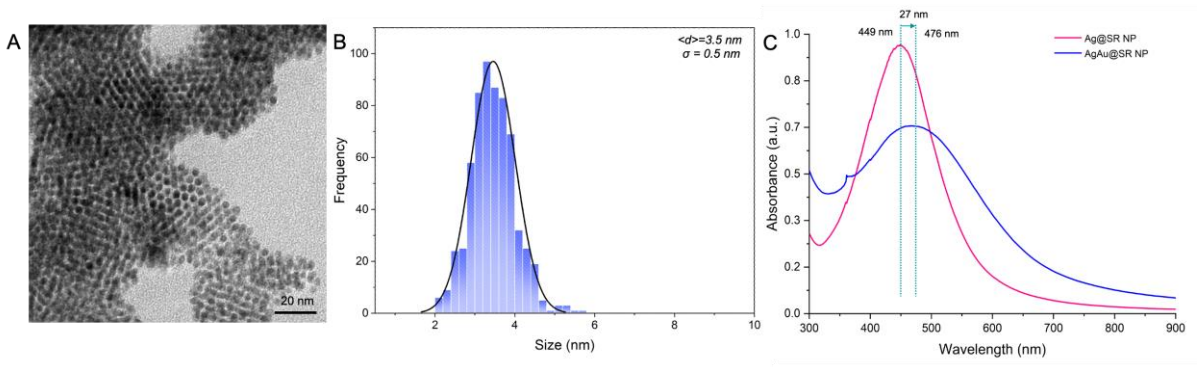

Fig. S3 Characterization of bimetallic AgAu@PET NPs. (A) TEM image, (B) particle size distribution, and (C) optical absorption spectrum (blue trace) of the reacted AgAu@PET NPs. The terms <d> and σ refer to mean diameter and standard deviation, respectively.

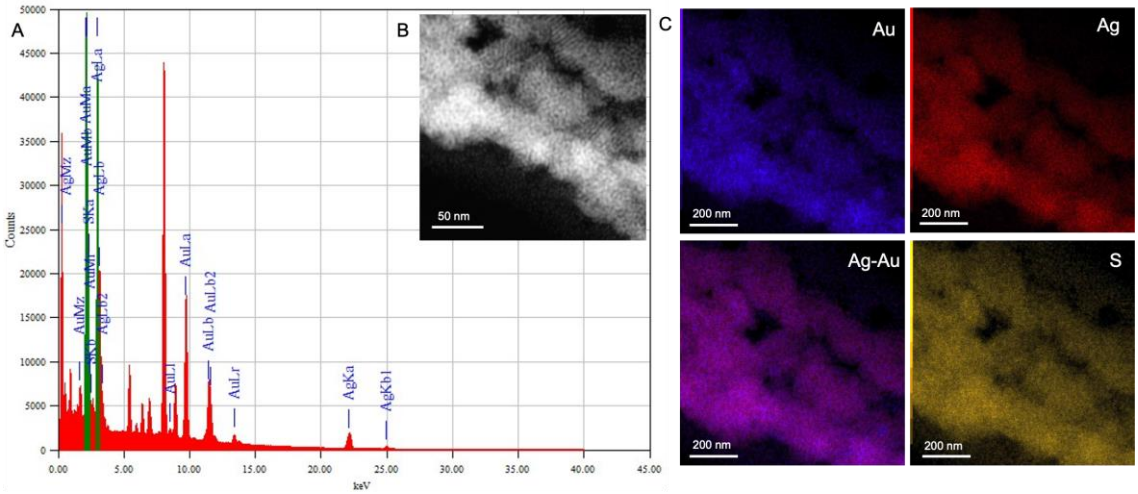

Fig. S4 Compositional analysis of reacted NPs. (A) EDS spectrum, (B) STEM image, and (C) the corresponding STEM-EDS elemental maps of the reacted NP.

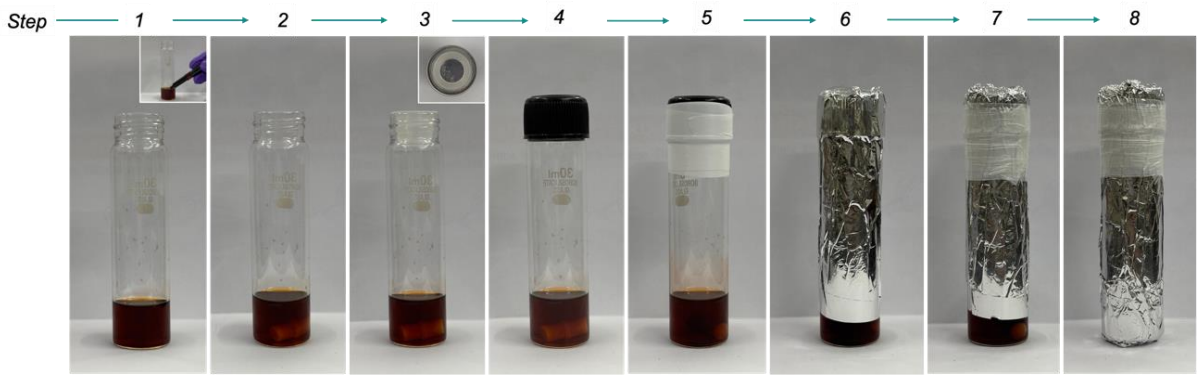

Fig. S5 Sequential of images demonstrating a step-by-step leak-proofing of the reaction setup so that it can handle the interparticle reaction for an extended period of time. In a glass vial, the reaction mixture was placed (step 1), and the total volume was marked for reference

(inset of step 1). A magnetic pellet was then added, and the reaction was ready for further processing (step 2). The vial was sealed with a stopper (step 3), a screw cap (step 4), and then secured with Teflon tape (step 5). An additional barrier against light and air was created by wrapping the vial with aluminium foil (step 6) and parafilm (step 7). The reaction bottles are now ready to be continuously stirred in the dark at 45 °C in an oil bath (step 7), and at room temperature (step 8).

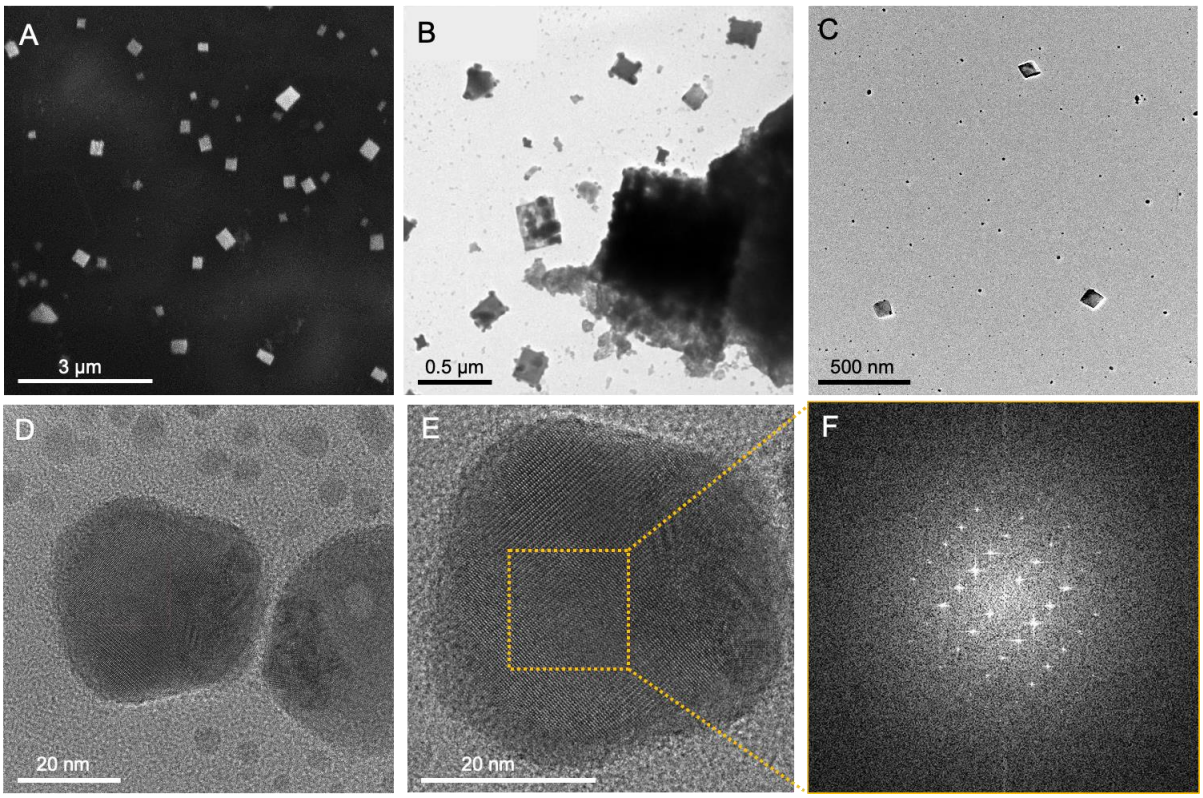

Fig. S6 FESEM (A), TEM (B, C), HRTEM (D, E), and the corresponding FFT (F) images of individual platelet-shaped nanocrystals, which are the building blocks of the cuboidal mesocrystals.

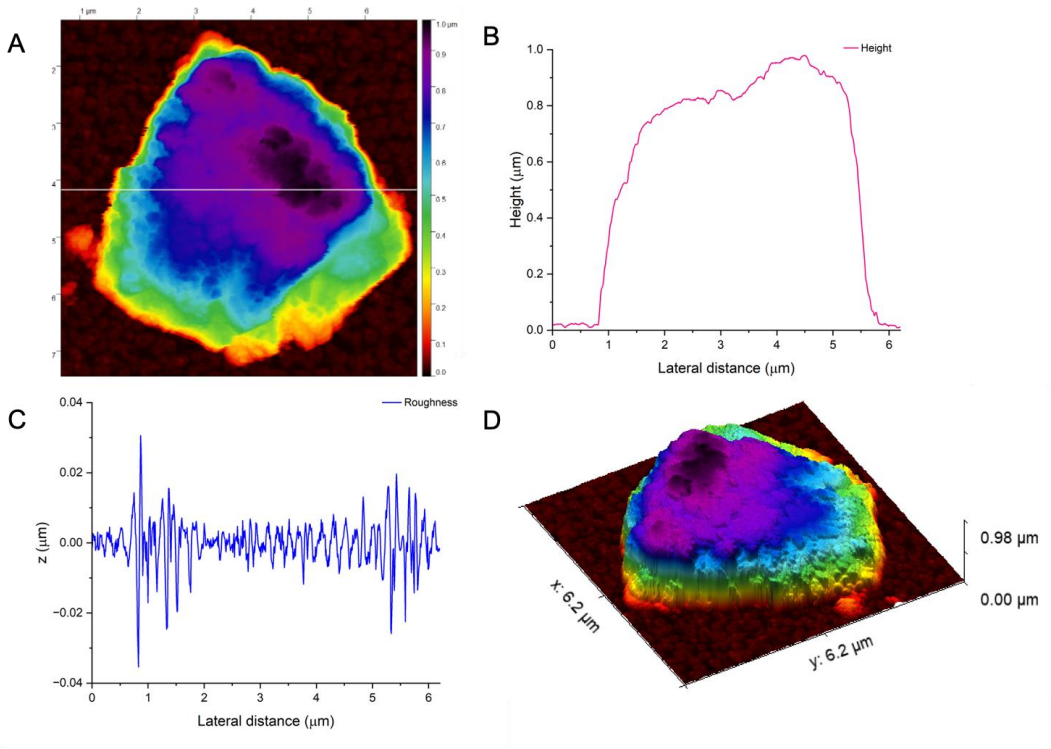

Fig. S7 AFM study of the mesocrystal obtained at the end of the interparticle reaction in Toluene at 45 °C. AFM image of one of the mesocrystals (A), and its corresponding height profile (B), roughness (C), and the 3D representation of the surface topology (D).

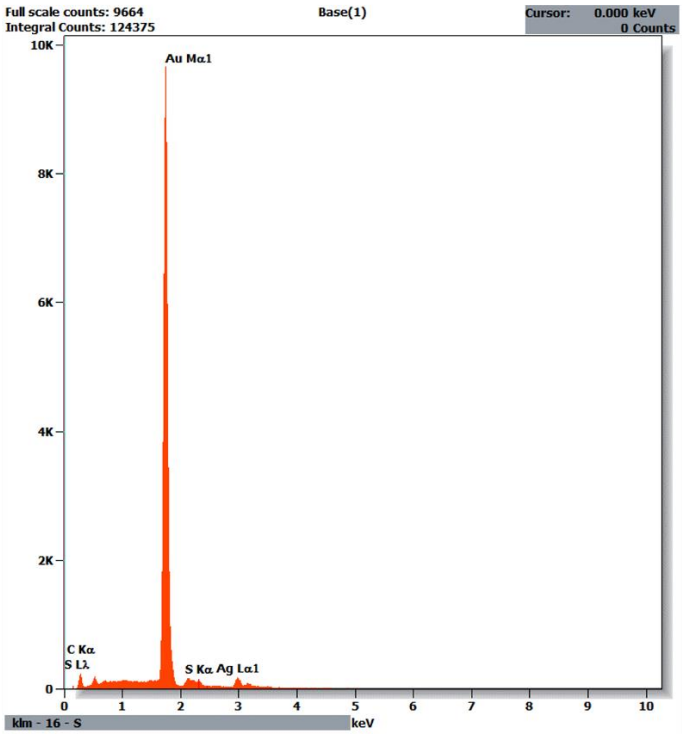

Fig. S8 EDS spectrum of the mesostructure produced by the interparticle reaction in toluene and under heating conditions.

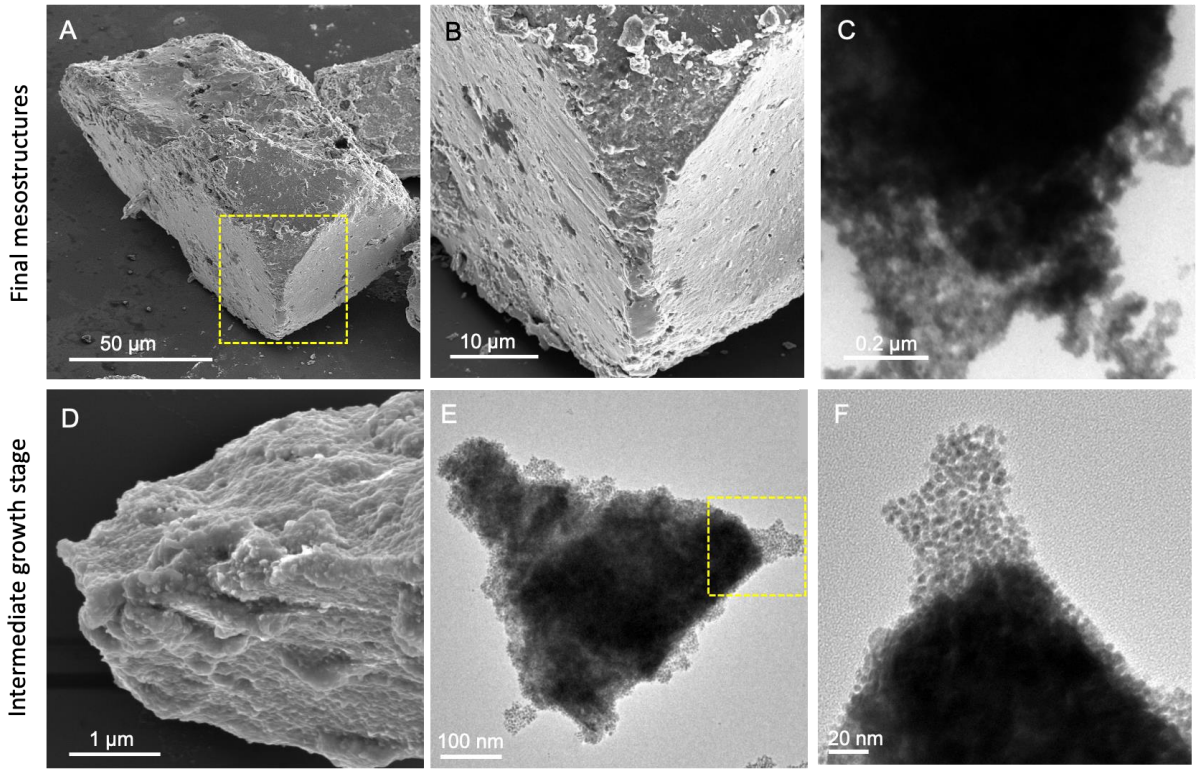

Fig. S9 Nucleation and growth of AgAu@PET NPs into random close-packed mesostructures. FESEM and TEM images of as-obtained mesostructure at the end of the reaction (A-C) and at the intermediate phase (D-F).

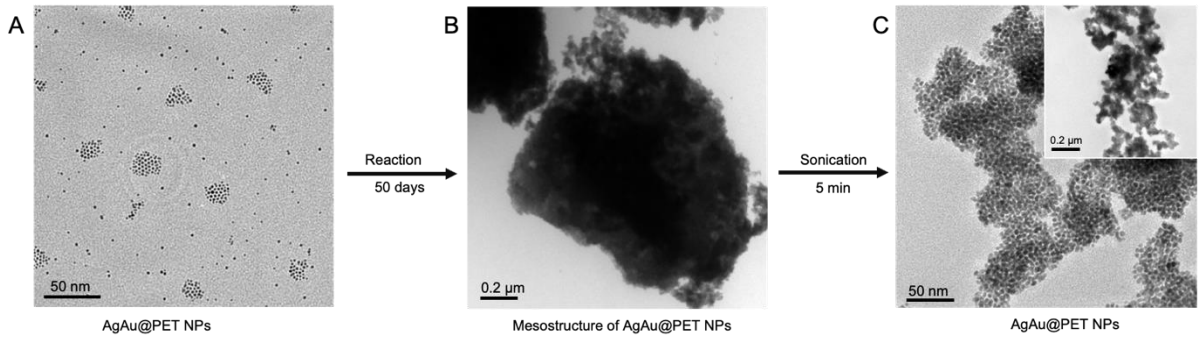

Fig. S10 TEM images of reacted AgAu@PET NPs before (A) and after assembly into a cuboidal mesostructure (B), and the recovered NPs after sonication (C). Inset (of C) shows the disintegration of larger mesostructure into original NP units.

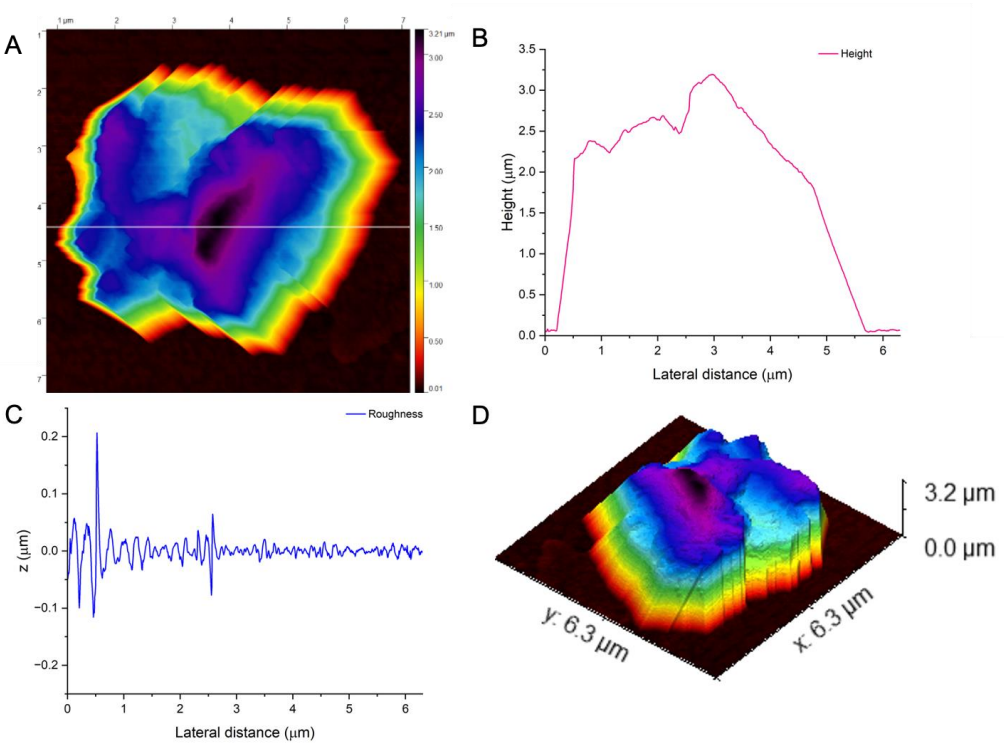

Fig. S11 AFM study of the mesostructure obtained at the end of the interparticle reaction in DCM at room temperature. AFM image of the mesostructure surface (A), and its corresponding height profile (B), roughness (C), and the 3D representation of the surface topology (D).

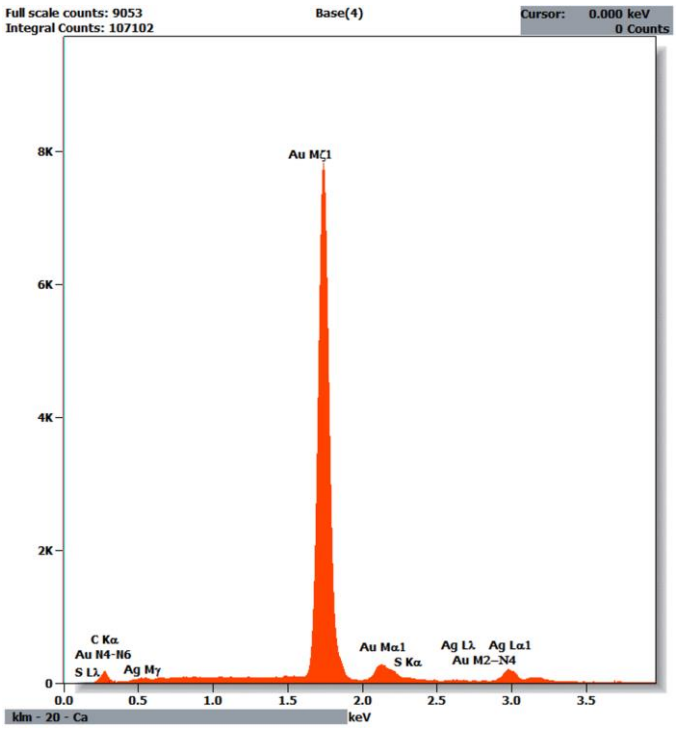

Fig. S12 EDS spectrum of the mesostructure produced by the interparticle reaction in DCM at room temperature.

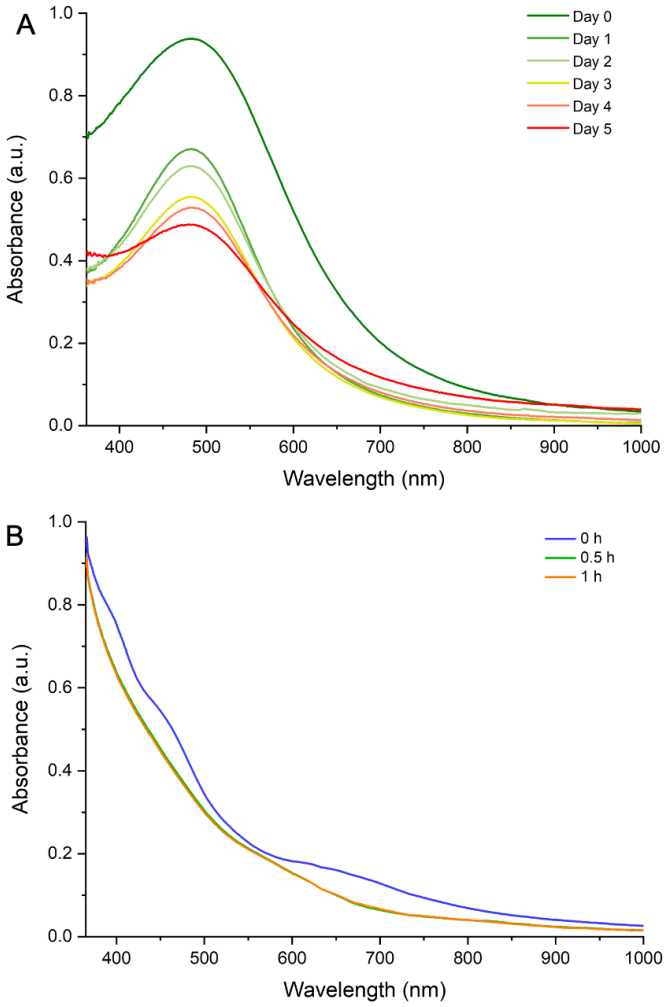

Fig. S13 Optical absorption spectra of the (A) parent polydispersed Ag@PET NPs, and (B) $[Au_{25}(PET)_{18}]^-$ NC, showing degradation over time when heated to 45°C in toluene with a constant stirring at 250 RPM.

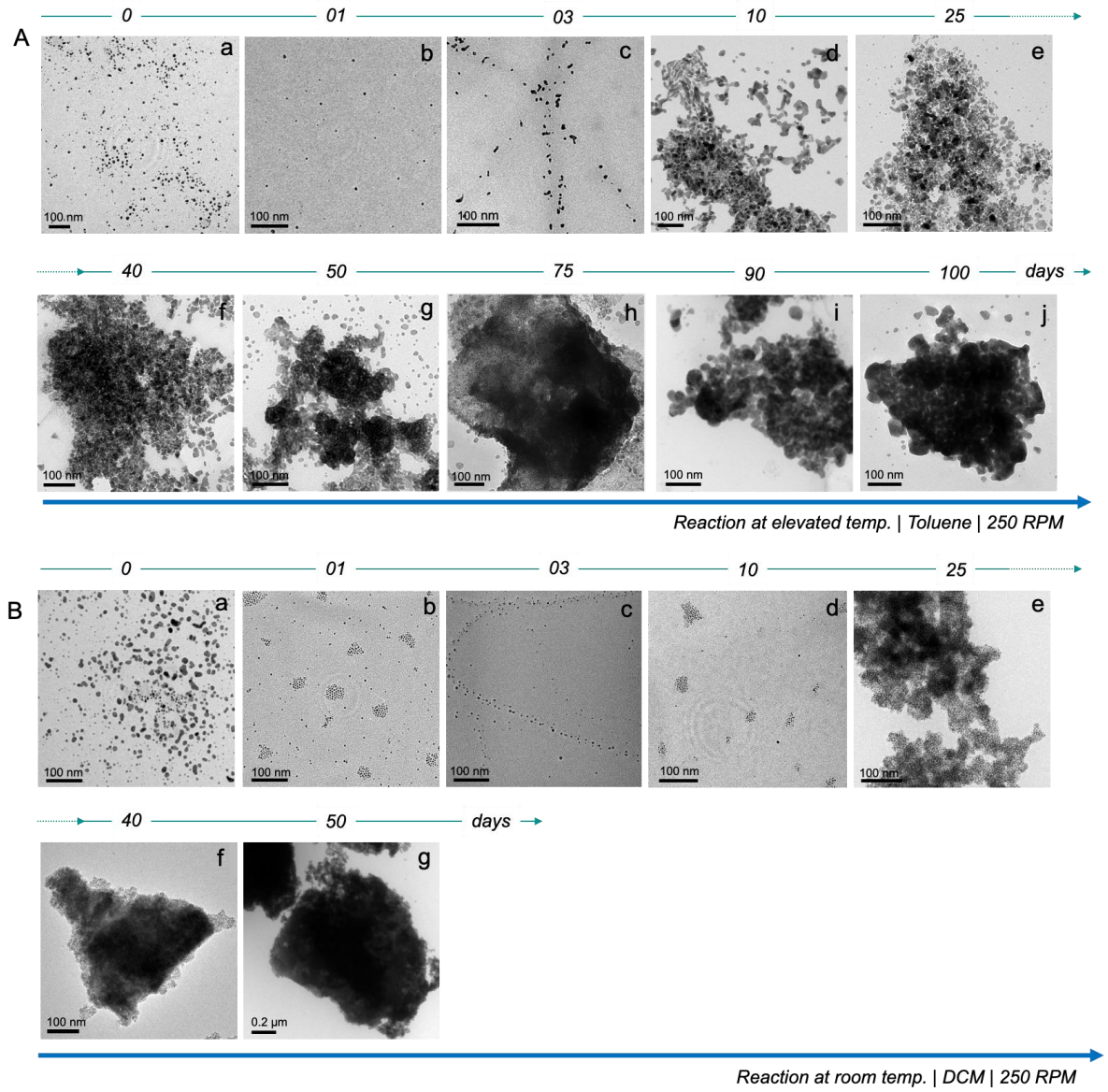

Fig. S14 TEM images showing time-dependent nucleation and growth of AgAu@PET NPs into the mesostructures when the interparticle reaction is carried out in toluene at 45°C (A) and in DCM at room temperature (B) with constant stirring at 250 RPM.

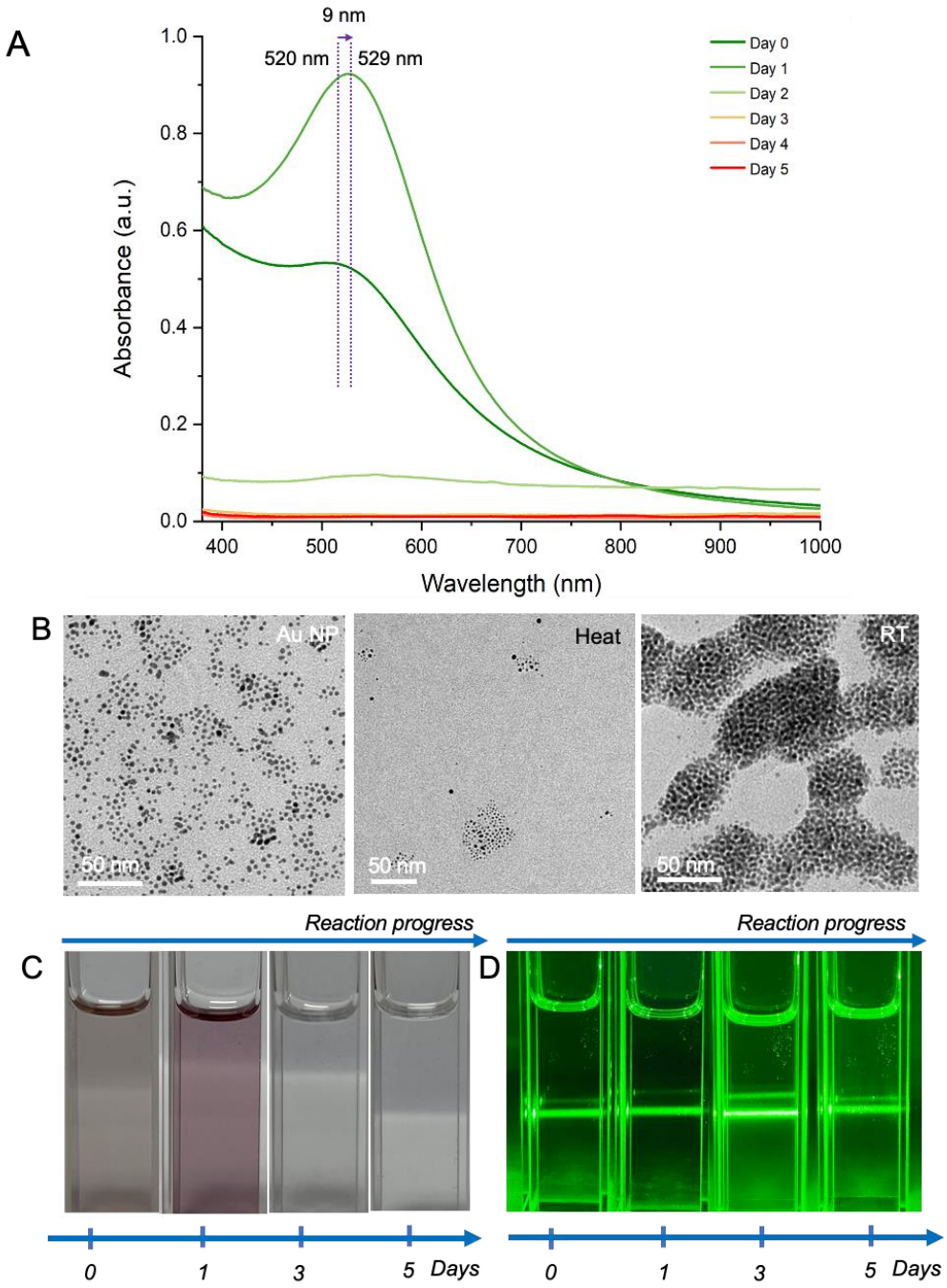

Fig. S15 (A) Time-dependent optical absorption spectra, (B) TEM images collected within a day, (C) photographic reaction progression, and (C) light scattering experiment with 630 nm laser light of interparticle reaction between Au@DMBT NPs and $[Ag_{25}(DMBT)_{18}]^-$ NC (Au NP−Ag NC). The particle mixture underwent degradation as the reaction was carried out at 45°C in toluene with constant stirring at 250 RPM (Heat in B). However, the particle mixture formed a stable assembly in DCM at room temperature (RT in B).

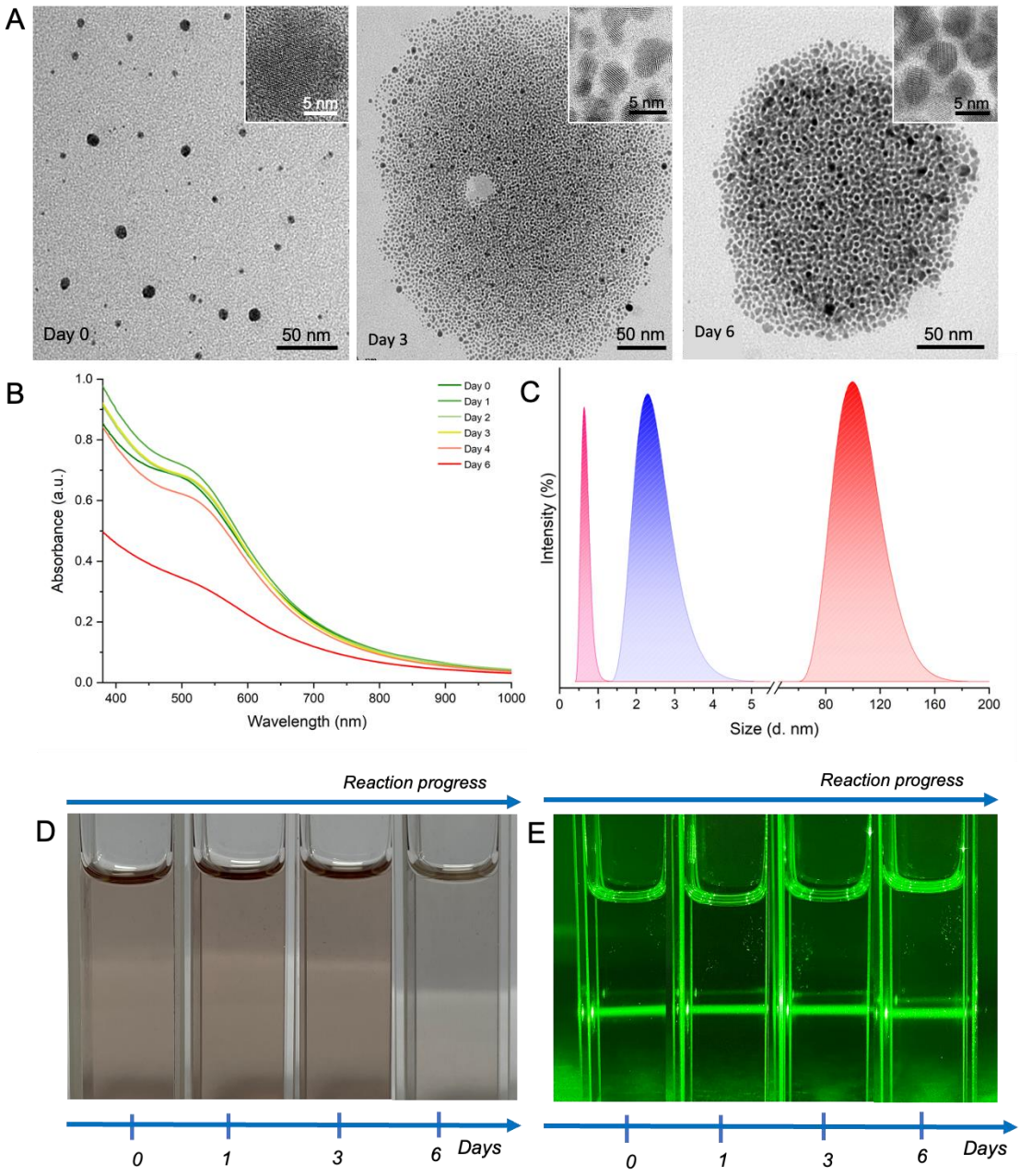

Fig. S16 Interparticle reaction between Au@PET NPs and $[Au_{25}(PET)_{18}]^-$ NC (Au NP−Au NC) as a function of time (A) TEM and HRTEM images, (B) optical absorption spectra, (C) size distribution measured in dynamic light scattering spectra, (D) photographic reaction progression, and (C) light scattering experiment with 630 nm laser light. The reaction was carried out in toluene at 45 °C with constant stirring at 250 RPM.

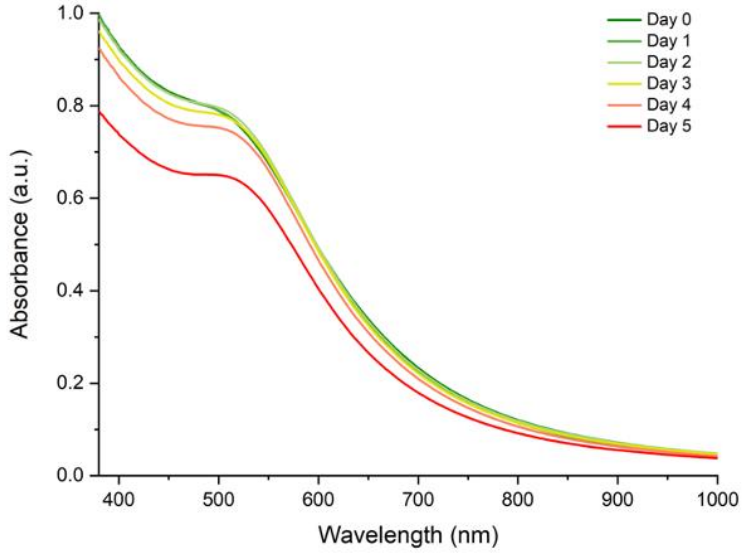

Fig. S17 Optical absorption spectra of the Au@PET NP dispersion in toluene with continual stirring at 250 RPM and heating at 45°C.

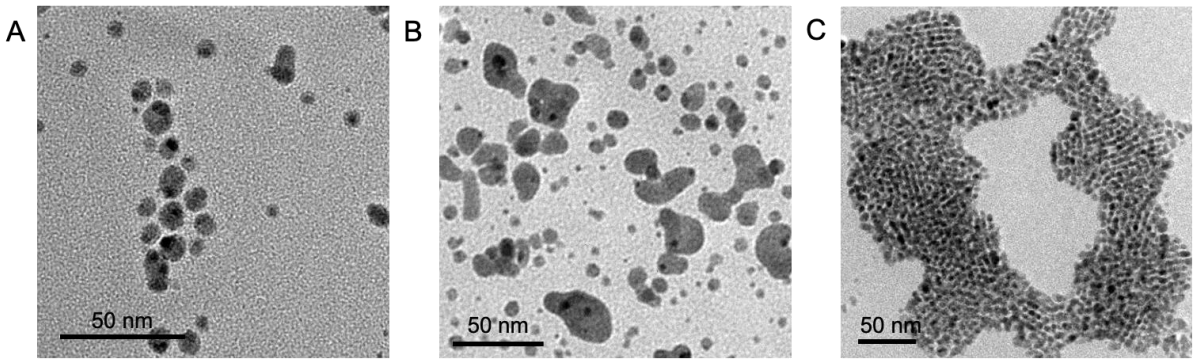

Fig. S18 TEM images show the parent Ag@PET NP (A) and its reaction with the $[Ag_{25}(DMBT)_{18}]^-$ NC (Ag NP−Ag NC) carried out at 45°C in toluene (B) and room temperature in DCM (C) with a constant stirring at 250 RPM.

References

1 J. Kimling, M. Maier, B. Okenve, V. Kotaidis, H. Ballot and A. Plech, *J. Phys. Chem. B*, 2006, **110**, 15700–15707.

2 P. Bose, P. Chakraborty, J. S. Mohanty, Nonappa, A. Ray Chowdhuri, E. Khatun, T. Ahuja, A. Mahendranath and T. Pradeep, *Nanoscale*, 2020, **12**, 22116–22128.

3 Z. Wu, J. Suhan and R. Jin, *J. Mater. Chem.*, 2009, **19**, 622–626.

4 C. P. Joshi, M. S. Bootharaju, M. J. Alhilaly and O. M. Bakr, *J. Am. Chem. Soc.*, 2015, **137**, 11578–11581.

5 M. Brust, M. Walker, D. Bethell, D. J. Schiffrin and R. Whyman, *J. Chem. Soc. Chem. Commun.*, 1994, 801–802.